3

Mutational analysis of the interaction between active site residues and the loop region in mammalian purple acid phosphatases

Enrico G. Funhoff, Jenny Ljusberg, Yunling Wang, Goran Andersson, and Bruce A. Averill.

Published in

Biochemistry 2001, 40(38), 11614-11622.

Abstract

Mammalian purple acid phosphatases (PAPs) can be divided in two groups, which exhibit distinct spectroscopic and kinetics properties: PAPs that consist of a single 36 kDa polypeptide; and PAPs that have undergone limited proteolysis to give two fragments with masses of 16 and 20 kDa, respectively. Proteolysis results in an increase in enzymatic activity, an increase in the optimal pH for activity, and a change in the g_z value of the characteristic EPR spectrum of the mixed valence binuclear iron center. It has been proposed that these changes are due to the loss of interactions between aspartate146 in an exposed loop region and active site residues upon proteolysis. In the present study, site directed mutagenesis of Asp146 in recombinant rat bone PAP (recRPAP) has confirmed this hypothesis. Conversion of Asp146 into Ala, which eliminates the interaction of the side chain with the active site, resulted in an enzyme with properties typical of PAPs isolated in proteolytically cleaved forms. The Asp146Asn and Asp146Glu mutants were also prepared and examined to assess the effects of altered electrostatic interactions and side-chain length.

Limited proteolysis of all three mutant enzymes with cathepsin L resulted in a significant increase in catalytic activity. Thus, although the interaction between aspartate146 and (an) active site residue(s) is the major factor responsible for the low catalytic activity of uncleaved PAPs, other interactions are also important. Since both *p*-NPP and osteopontin, a potential *in vivo* substrate, show the same level of activation, the observed increase in catalytic activity upon proteolysis is likely to be due to electrostatic than steric effects. EPR spectra of FeZn-recRPAP before and after cleavage by cathepsin L suggest that cleavage primarily affects the divalent metal site. The observation that $pK_{es,1,}$ is also sensitive to changes at the divalent site is consistent with the proposal that the nucleophilic hydroxide is that bridging the divalent and trivalent metals.

Introduction

The iron-containing purple acid phosphatases (PAPs) are found in mammalian, plant, fungal and bacterial sources (*1, 2*). Mammalian PAPs contain an FeFe active site and typically are single polypeptide proteins with a molecular mass of 36 kDa. In contrast, plant PAPs contain either an FeZn or FeMn metal center and are typically dimers of 55 kDa subunits. (*2, 3*). Although the similarities in their primary sequences are modest, the active site structure and the residues coordinating the active site are identical in mammalian and plant PAPs. A recent search of the genomic databases, however, identified new PAP sequences in plants that are not homologues of the known plant PAPs, but which have a predicted molecular mass of 35-40 kDa, and appear to be more closely related to the mammalian PAPs (*4*).

In most cases, the specific physiological function of PAPs is not yet clear (*5*). In pigs, PAP apparently functions in the transport of Fe to transferrin (*6, 7*). In general, PAPs exhibit a broad hydrolytic activity towards phosphate esters in vitro (*8, 9*), pointing to a degradative function in PAP-expressing cells such as bone marrow cells and macrophages. Studies on PAP "knockout" mice show that the enzyme is essential for normal bone resorption and mineralization in developing bones (*10*). Overexpression of PAP in mice results in increased resorption of trabecular bone and mild osteoporosis (*11*). The recent demonstration that PAP is also present in dendritic cells suggests that PAP may function in regulating intracellular signaling pathways that control trafficking of MHC Class II-containing vesicles involved in antigen presentation (*12*). Osteopontin, a phosphoprotein that has been proposed to be the *in vivo* substrate of PAP, is apparently involved in both bone degradation and the immune system (*13, 14*), consistent with a relationship between PAP activity and the immune response.

The X-ray structure of kidney bean PAP showed that the active site contained a zinc ion coordinated by two histidines and an asparagine, and a ferric ion coordinated by a tyrosine, a histidine and an aspartate residue (*15*). The two metal ions are bridged by a hydroxide and an aspartate carboxylate (schematic representation, Figure 3.1). Crystal structures of three mammalian PAPs (single polypeptide uteroferrin, Uf, at 1.5 Å resolution (*16*) and recombinant rat bone PAP, recRPAP, at 2.2 Å (*17*) and 2.7 Å resolution (*18*)) have recently been reported. All three proteins have highly symmetrical structures consisting of 4 α-helixes coupled by ß-sheets. The active site is found at the top of the protein in the vicinity of two exposed loops (residues 18 to 24 and 145 to 160; numbering according to the human sequence (*38*)); The latter is absent in the 2.7 Å resolution rat bone structure, although the residues coordinating the metal center are completely conserved in all mammalian PAPs. One of the residues proposed to interact with substrate differs in plant and mammalian PAPs: His295 in the former is replaced by Glu194 in the latter (*15, 19*). The residues coordinated to the binuclear active site of the regulatory Ser/Thr protein phosphatases (PPs) are essentially identical to those in PAPs (*20-23*), as previously proposed based on the presence of a phosphoesterase motif (*24*). PPs, however, lack the tyrosinate coordinated to the Fe^{3+} metal ion that is responsible for the purple color, and instead contain a solvent molecule coordinated to the Fe^{3+}. The amino acids that interact with substrate in the PPs are one histidine (His92, according to the human sequence), which is conserved in all PAPs and PPs, and two arginines. Based on the high degree of similarity between the active sites of PAPs and PPs, it seems likely

Figure 3.1: Schematic representation of the active site of mammalian PAPs including the interactions discussed in this chapter, with numbering according to the human sequence.

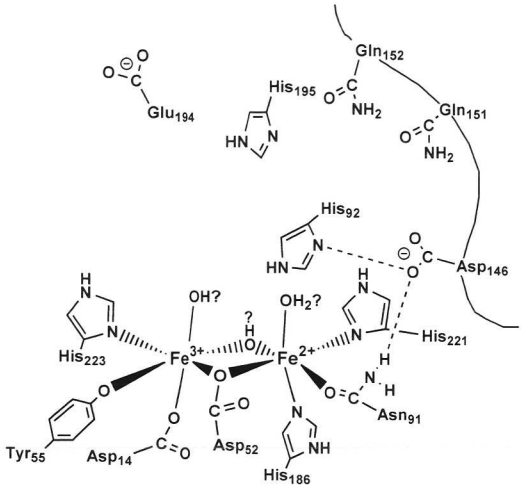

that both enzymes utilize similar mechanisms (for an extensive review on PP2B, see Rusnak et al. (*25*)).

Mammalian PAPs are known to be activated by proteolytic cleavage. For example, BSPAP is activated 4-fold at pH 6.0 by trypsin cleavage (*26*), while an 8-fold increase in activity at pH 5.8 is found for recRPAP (*9*) treated with cysteine proteases such as cathepsin B. Trypsin cleavage of recombinant human PAP (recHPAP) results in a 4-fold activation, when activity at the optimal pH for both the intact and proteolytically cleaved forms is compared (*27*). Activation is accompanied by a shift in pH optimum, from 4.8 to 5.9 for recRPAP and from 5.5 to 6.3 for recHPAP (*9, 27*). Proteolytic cleavage also converts the EPR spectrum from one that is characteristic of single polypeptide PAPs (with features at g_{xyz} = 1.58, 1.73, and 1.94) into one characteristic of proteolytically cleaved PAPs (with features at g_{xyz} = 1.60, 1.73, and 1.86 at pH 5.0 as observed for recHPAP). In addition, mass spectrometric studies on recHPAP (*27*) and SDS-PAGE studies of recRPAP (*9*) showed that proteolytic cleavage excises a portion of a highly exposed loop near the active site. It has been proposed that the differences in both kinetics and spectroscopic characteristics reported for mammalian PAPs are due to changes in interactions between the loop and the active site upon cleavage (*27*).

Careful examination of the structures of Uf and recRPAP suggested that two major interactions between the loop and the active site could be responsible for the observed differences between intact and proteolytically cleaved PAPs: that between Asp146 and either Asn91 or His92, both of which are conserved active site residues in all PAPs and PPs (*27*). Proteolytic cleavage would result in the loss of interaction between Asp146 and Asn91, destabilizing a Asn91 resonance structure which contains a C-N double bond and a polarized carboxylate oxygen which is a better metal ligand. Thus, upon proteolysis the Lewis acidity of the divalent metal ion would increase with a concomitant increase in the electrophilicity of the enzyme-bound substrate (assuming that the substrate coordinates to the divalent metal ion).

In the present study, we prepared mutants of Asp146 to explore the molecular basis for the relationship between proteolytic cleavage and enzymatic activation. Kinetics and spectroscopic characterization of the mutants demonstrated that interactions between Asp146 and the active site are primarily responsible for the differences observed between single polypeptide and proteolytically cleaved forms of PAPs. Limited proteolysis of the mutant enzymes showed that further activation was possible, suggesting the presence of additional interactions between the loop residues and the active site that affect catalytic activity. Finally, the properties of the FeZn form of wild-type recRPAP, before and after cathepsin L cleavage, suggest that the interaction between Asp146 and Asn91, which primarily affects the divalent metal site, is likely to be more important than that between Asp146 and His92, which primarily affects the trivalent metal site.

Experimental procedures

Materials

Restriction enzymes, DNA purification system, Cellfect™, and the baculovirus expression system were purchased from Life Technologies. Excell 405™ SFM (JRH Bioscience), *p*-NPP (Fluka), and cathepsin L (219402, Calbiochem (CH)) and all other chemicals were of the highest purity commercially available.

General procedures

Enzyme concentrations were determined by measuring the absorbance of the Tyr^{-}- to-Fe^{3+} charge transfer at λ_{max} (510-550 nm, depending on the form; ε=4080 $M^{-1}cm^{-1}$) on a Cary 50 spectrophotometer.

Recombinant baculovirus stocks containing coding regions for recRPAP or the D146A, D146E and D146N mutants were used to infect High 5 cells cultured in 500-1000 ml Excel 405™ SFM at 27°C; the cell density was 0.8×10^6 cells/ml, and a low MOI (0.001-0.01) was used. After 6 days the cells were removed by centrifugation (10.000×g), and the enzyme was purified from the medium.

For the preparation of FeZn-recRPAP, metal-free buffer was prepared by passing it through a Chelex-100 column. A Sephadex G-25 column was eluted with a solution containing 5 mM ascorbic acid and 1 mM o-phenanthroline to remove excess metals, and subsequently eluted with metal free Millipore water and a metal-free solution containing 40 mM Na-acetate buffer, 1.6 M KCl, and 20% glycerol in Millipore water.

Generation of recRPAP mutants

Rat PAP cDNA (1.4 kb (*29*)) was cloned into a pCMV5 vector, and site-directed mutagenesis was performed using the 5'—>3' MORPH site-specific plasmid DNA mutagenesis kit (5 Prime —> 3 Prime Inc., Boulder, CO). Primers used for each specific mutation were as follows: D146E, primer: 5'-GCAATTCCGAAGACTTTGTCAG-3; D146A, 5'-GTGGCAATTCCGCCGACTTTGTCAG-3'; D146N, 5'-GCAATTCCAACGACTTTGTCAG-3'. The underlined bases indicate changes compared to the wild-type sequence. The primers employed for mutagenesis were phosphorylated by T4 kinase according to the manufacturer's instruction. DNA sequencing of the recRPAP mutants was used to verify the sequence (Cybergene AB, NOVUM, Huddinge, Sweden). Wild-type or mutant RPAP

cDNAs were cloned into the baculovirus expression vector pFASTBAC1 donor plasmid using the EcoRI restriction site. The proper orientation was determined by PstI cleavage, and confirmed by DNA sequencing. The pFASTBAC1 donor vectors containing wild-type or mutant RPAP cDNAs were transformed into DH10Bac cells for homologous recombination with bacmid. Recombinant bacmids were selected by Luria Agar plates containing antibiotics and IPTG (50 µg/ml kanamycin, 7 µg/ml gentamycin, 10 µg/ml tetracycline, 100 µg/ml Bluo-gal and 40 µg/ml IPTG) and confirmed by PCR. Bacmid DNA of wild-type recRPAP and mutants was used to transfect High 5 cells in the presence of Cellfect™ to prepare recombinant baculovirus, as described in the instruction manual of the bac-to-bac system of Life Technologies. The virus was amplified before use.

Purification of wild-type and mutant enzymes

Purification of wild-type recRPAP, and the D146N, D146E, and D146A mutants was performed as described previously for recHPAP (*27*), with the exception that hydrophobic interaction chromatography was performed at pH 6.9 in MES buffer. Since wild-type recRPAP was found to be partly cleaved (10-15%) after purification, an additional FPLC step was used. RecRPAP was loaded onto a Pharmacia Mono S column preequilibrated with 50 mM MES pH 6.5, 0.1M KCl. The protein was eluted with 20 ml of a 0.1 to 0.5 M KCl gradient. Intact recRPAP was eluted at approximately 0.2-0.25 M KCl.

SDS-PAGE analysis

SDS-PAGE was performed under reducing conditions essentially as described by Laemmli (*30*). Gels were either stained with Coomassie or blotted to immuno-PVDF membranes and probed with rabbit anti-recRPAP antiserum (diluted ×100) as the primary antibody and alkaline phosphatase-conjugated goat anti-rabbit IgG (diluted ×500) as the secondary. Development was performed with NBT/BCIP. All steps were performed in accordance with the manufacturer's protocols.

Kinetics measurements

Enzyme assay: Enzymatic activity was determined by monitoring the formation of the *p*-nitrophenolate anion at 410 nm (ε_{410nm}=16.6 $mM^{-1}cm^{-1}$) in a buffer containing 50 mM MES (pH 6.0), 300 mM KCl, 10 mM Na-K tartrate, 6.7 mM Na-ascorbate, 0.37 mM $Fe(NH_4)_2(SO_4)_2$ and 50 mM *p*-NPP at 22°C. At intervals after enzyme addition, 250 µl aliquots were removed and quenched with 1.0 ml of 0.5 M NaOH to convert all product to the phenolate form. The intact and proteolytically cleaved FeZn form of recRPAP were assayed in the absence of Na-ascorbate and $Fe(NH_4)_2(SO_4)_2$.

pH dependence: The pH dependence of k_{cat} was measured in 100 mM buffer (Na-acetate, MES or HEPES), 300 mM KCl, 10 mM Na-K tartrate, 6.7 mM Na-ascorbate, 0.37 mM $Fe(NH_4)_2(SO_4)_2$, and *p*-NPP concentrations varied between 0.5 and 50 mM. For each determination of V_{max} and K_M, the hydrolysis rate was measured at 6 different *p*-NPP concentrations. After each assay, the pH of the reaction mixture was measured to ensure that it had not changed. Values of K_M and V_{max} were obtained by non-linear regression using the program EnzymeKinetics (Trinity Software).

Proteolytic activation: Phosphatase activity was assayed in 96-well plates with *p*-NPP as substrate in 150 µl incubation medium, pH 5.8, with final concentrations: 50 mM *p*-NPP, 1 mM ascorbic acid, 0.1 mM $Fe(NH_4)_2(SO_4)_2$, 0.1 M Na-acetate, 0.15 M KCl, 10 mM Na-

tartrate, 0.1 % (v/v) Triton X-100. The *p*-nitrophenol liberated after 1h of incubation at 37°C was converted to *p*-nitrophenolate by addition of 100 µl 0.3 M NaOH, and the absorbance was measured at 405 nm (ε_{405}=18.9 $mM^{-1}cm^{-1}$) with a Spectramax 250 spectrophotometer (Molecular Devices, Sunnyvale, CA, USA).

Osteopontin: Enzyme assays with bovine milk osteopontin as substrate were performed essentially as described by Baykov et al (*31*). Osteopontin (2-8 µM) was dissolved in the same buffer as used for the *p*-NPP assay, except the pH was 5.0 (total incubation volume 50 µl). The assay was stopped after 1 h at 37°C by the addition of 50 µl color reagent (0.12 % malachite green in 3 M H_2SO_4, 7.5% ammonium molybdate, and 11% (v/v) Tween-20 [10:2.5:0.2 by volume]). A phosphate curve (0-4 nmol) was always run in parallel. After color development for 30 minutes, the absorbance was read at 630 nm with a Spectramax 250 spectrophotometer.

Electron paramagnetic resonance (EPR) spectroscopy

Samples contained 20 % glycerol (v/v), and were frozen in liquid N_2. X-band EPR spectra (9.43 GHz) were obtained on a Bruker ECS106 EPR spectrometer equipped with an Oxford Instruments ESR900 helium-flow cryostat with an ITC4 temperature controller. The magnetic field was calibrated with an AEG Magnetic Field Meter, and the frequency was measured with a HP 5350B Microwave Frequency Counter.

Preparation of zinc-substituted recRPAP

Half apo-recRPAP was prepared as previously prescribed for BSPAP (*32*). To 1 ml of 60 µM FeFe recRPAP in 40 mM Na-acetate buffer, pH 5.0, 1.6 M KCl, and 20% glycerol, 1 mM o-phenanthroline and 5 mM freshly prepared sodium dithionite were added. The release of Fe^{2+} was monitored by the absorbance of the $[Fe(phen)_3]^{2+}$ complex at 510 nm. After 3 minutes the half apo-enzyme was separated using a Sephadex G-25 column, which was eluted with a Chelex-treated 40 mM Na-acetate buffer, pH 5.0, containing 1.6 M KCl and 20 % glycerol. For reconstitution, the sample was incubated with a 20-fold excess of $ZnCl_2$ at room temperature for 5 hours, followed by incubation overnight at 4°C. The enzyme sample was concentrated/diluted with 50 mM Na-acetate (pH 5.0), 2 M KCl, to remove excess metal ions using a Centricon-30 concentrator. Enzymatic assays and EPR measurements under reducing and oxidizing conditions confirmed that at most insignificant amounts of FeFe-recRPAP were present. The enzyme was used without further purification.

Proteolytic digestion of recRPAP

Small-scale procedure: RecRPAP (wt, D146E, D146A, or D146N) was digested with cathepsin L at 37°C for 2h with final concentrations: PAP, 7 ng/µl; cathepsin L, 3 µU/µl; 50 mM Na-acetate; 1 mM EDTA; and 2 mM DTT, pH 5.5. Cathepsin L was pre-reduced in 2 mM DTT for 7 min before it was added to the incubation solution. Trypsin (Sigma T-8003) digestion of recRPAP (wt, D146E, D146A, or D146N) was performed at room temperature for 45 min with final concentrations: PAP, 7 ng/µl; trypsin, 49.5 U/µl; 50 mM Tris-HCl, pH 7.5; 0.1 M NaCl; and 10 mM $CaCl_2$. Proteolytic digestions were stopped with proteinase inhibitor cocktail Complete (Roche) in accordance with the manufacturer's instructions.

Large-scale procedure: 120 µl Pre-reduced (7 mM DTT, 1 mM EDTA) cathepsin L (354 µg/ml) was added to 1 ml solution (40 mM Na-acetate, pH 5.0) containing 2.1 mg/ml FeZn recRPAP, 0.5 mM DDT, and 0.5 mM EDTA. After 2 hours at room temperature the sample was maintained at 4ºC overnight. Cathepsin L and other reagents were removed by repeated concentration/dilution using a Centricon (30 kDa cut off).

Figure 3.2: Fragmentation pattern after cathepsin L cleavage of recombinant RPAP.

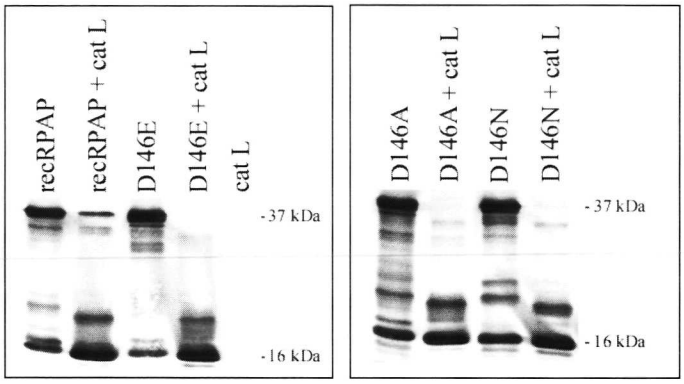

Results

Production of wild-type recRPAP and the three mutants by baculovirus-infected High 5 cells was followed by activity measurements. At 6 days post infection the activity was consistent with the presence of 6-12 mg enzyme per liter, and the culture was stopped. Purification of the four enzymes gave protein samples with R values (A_{280}/A_{515}) of 16-20, and a single band corresponding to single polypeptide PAP was observed for the mutants by SDS-PAGE under reducing conditions stained with coomassie (not shown). Western blots (Figure 3.2) after kinetics and spectroscopic characterization revealed that small amounts of proteolytically cleaved enzyme were present. The purified wild-type recRPAP contained 10-15% proteolytically cleaved protein, which was separated from the intact form using an additional Mono S cation exchange chromatography step (*9*). UV-VIS spectroscopy of both wild-type enzyme and the mutants showed a maximal absorption at 515 nm (λ_{max}).

Reported pH optima for mammalian PAPs range from 4.7 to 6.3 (*9, 27, 33*). RecRPAP showed a non-gaussian pH optimum near 4.7, which shifted to 5.8 upon proteolytic cleavage (*9*). Similarly, early studies on BSPAP reported an optimal pH of 5.9 (*50*). These studies were, however, performed at a single non-saturating substrate concentration, which can result in an apparent pH optimum that is significantly lower than the actual value. For example, measuring the pH optimum of single polypeptide Uf at high *p*-NPP concentrations gives a pH optimum that is 0.4 units higher than reported (M. Pinkse, M. Merkx, B.A.A. Averill, unpublished results), while more detailed studies gave a pH optimum of 6.5 for BSPAP (*29*). We therefore analyzed the pH dependence of k_{cat} of the wild-type and mutant recRPAPs by measuring V_{max} over the pH range 4 to 8.

Figure 3.3: pH dependencies of k_{cat}, k_{cat}/K_M and K_M for wild-type (A) and mutant Asp146Asn (B), Asp146Glu (C), and Asp146Ala (D) recRPAP with *p*-NPP as substrate at 22°C. The lines represents fits of k_{cat} and k_{cat}/K_M to the rapid equilibrium diprotic model. The derived kinetics constants are depicted in the table.

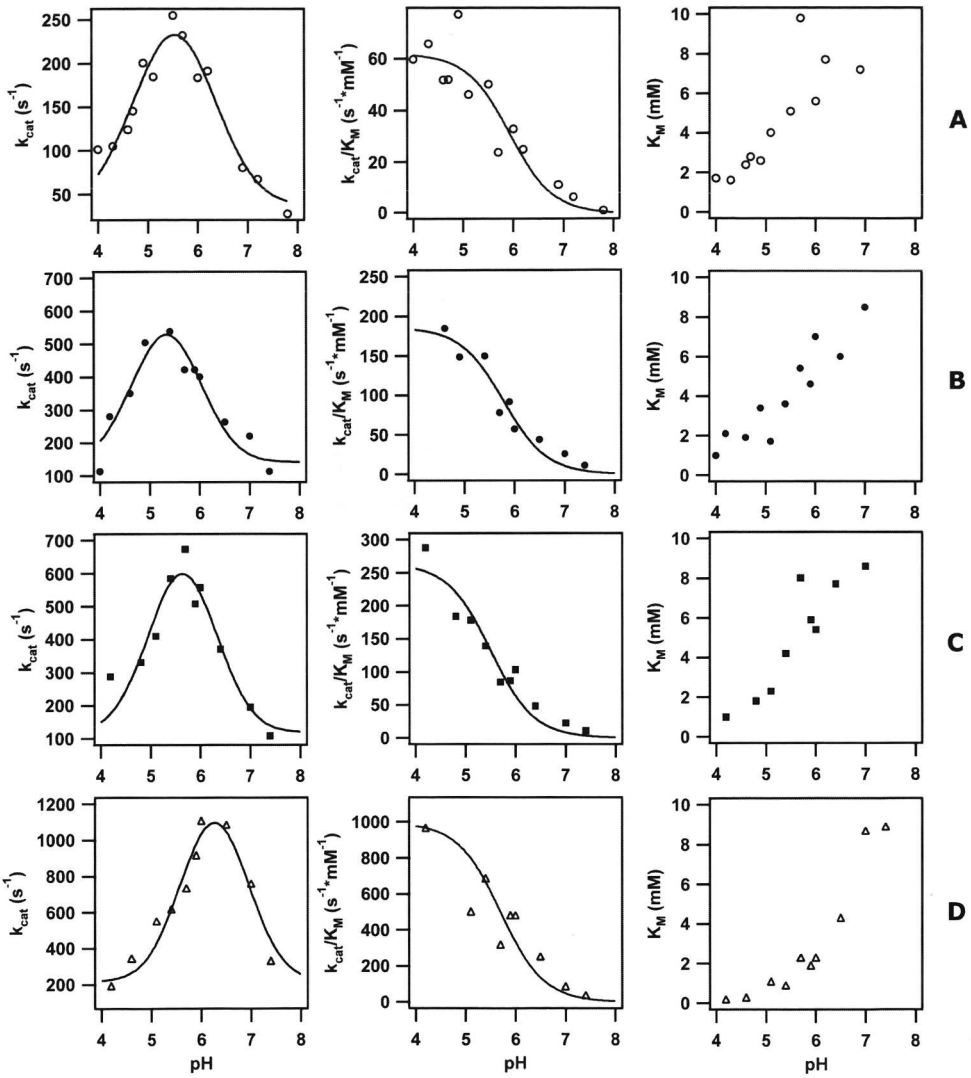

	pH_{opt}	k_{cat} (s^{-1})	$pK_{es,1}$ [a]	$pK_{es,2}$ [a]	$pK_{e,2}$ [b]
RecRPAP	5.5	240	4.5	6.6	5.6
D146N	5.4	530	4.3	6.6	5.8
D146E	5.7	710	4.9	6.5	5.5
D146A	6.3	1310	5.5	7.1	5.7

k_{cat} is defined as the number of substrate molecules hydrolyzed per enzyme molecule per second; $pK_{es,1}$ and $pK_{es,2}$ are for deprotonation/protonation events of a group of the enzyme-substrate complex; and pK_{e2} is for a deprotonation/protonation event of a group of the enzyme. K_S is defined as the dissociation constant of the ES complex.

[a] Obtained from a fit of $k_{cat,obs}$ as a function of pH.

[b] Obtained from a fit of $k_{cat,obs}/K_{M,obs}$ as a function of pH with $pK_{e1}<2$.

The pH dependencies were analyzed according to a rapid equilibrium diprotic model (*34*), for which the following expressions were derived for the k_{cat}, and k_{cat}/K_M (assuming that all equilibria are fast compared to k_{cat}).

$$k_{cat(obs)}=k_{cat}/(1+[H^+]/K_{es,1}+K_{es,2}/[H^+]) \quad (a)$$

$$k_{cat(obs)}/K_{M(obs)}=k_{cat}/K_S(1+[H^+]/K_{e1}+K_{e2}/[H^+]) \quad (b)$$

The pH optima and pK_a values obtained by fitting the data are given in Figure 3.3. RecRPAP has a gaussian pH optimum near pH 5.5, which is substantially higher than previously reported (pH 4.7) (*9*). The pH optima of the D146E (5.7) and D146A (6.3) mutants are higher, due to a shift of $pK_{es,1}$ from 4.5 to 4.9 and 5.5, respectively. Except for the D146A mutant ($pK_{es,2}$ = 7.1), the value of $pK_{es,2}$ is constant at around pH 6.6. k_{cat} for the mutants was up to five times greater than that of the wild-type enzyme (cf. 240 s^{-1} for recRPAP vs. 1310 s^{-1} for the D146A mutant, at their respective pH optima). Although the pK_a values for the D146N mutant are not significantly different from those of the wild-type enzyme, k_{cat} is twice as large for the mutant. The D146E mutant showed a greater increase in k_{cat} (710 s^{-1}) compared to D146N (530 s^{-1}). Fitting of the k_{cat}/K_M values of all four forms using a single pK_a showed no significant change in $pK_{e,2}$. The K_M values of the mutants do not vary significantly.

Mammalian PAPs isolated as single polypeptide or proteolytically cleaved proteins exhibit characteristic EPR spectra. Typically, uncleaved proteins have a g_z value around 1.94, which is shifted to 1.86 in the proteolytically cleaved proteins (*35-37*). As reported earlier (*29*), the EPR spectrum of intact wild-type recRPAP at pH 5.0 (Figure 3.4) has apparent g-values of 1.97 (with a shoulder at 1.94), 1.73 and 1.61. In the D146A mutant, where the interaction between Asp146 and Asn91 and/or His92 has been abolished, the g_z value was shifted to 1.86 and g_x to 1.58; some broadening of the EPR signal was also observed. The spectrum of the D146E mutant resembled that of a

Table 3.1: Activity[a] of wild-type (wt) recRPAP and D146 mutants after proteolytic digestion.

	Spec. Act.[b] (U mg^{-1})	k_{cat}[b] (s^{-1})	Activation[c] (vs. wt recRPAP)	K_M (mM)	k_{cat}/Km (10^3 M^{-1} s^{-1})	Activation[d] (vs. wt recRPAP)
wt recRPAP	459 (41)	268 (24)	1	3.4	79	1
+ cat L	3617 (269)	2108 (157)	7.9	1.1	1916	24.2
+ Trypsin	1303 (44)	759 (26)	2.8	2.0	271	3.4
D146N	673 (97)	393 (57)	1.5	3.1	127	1.6
+ cat L	3310 (327)	1929 (191)	7.2	1.1	1754	22.2
D146E	1551 (53)	904 (31)	3.4	3.2	283	3.6
+ cat L	4205 (141)	2450 (82)	9.1	0.9	2722	34.5
D146A	2406 (85)	1402 (49)	5.2	2.1	668	8.5
+ cat L	4225 (191)	2462 (111)	9.2	1.0	2462	31.2
+ Trypsin	1712 (91)	998 (53)	3.7	1.4	713	9.0

[a] Activity measurements were performed with *p*-NPP as substrate as described in the experimental section under "kinetics measurements; proteolytic activation".
[b] Numbers in parentheses are standard deviation values.
[c] times activation of k_{cat}
[d] times activation of k_{cat}/K_M

Figure 3.4: EPR spectra of single polypeptide wild-type and mutant recRPAP at pH 5.0. EPR conditions: microwave power 2mW; microwave freguency, 9.42 GHz; modulation, 12.7 G at 100 kHz; temperature, 4.6 K.

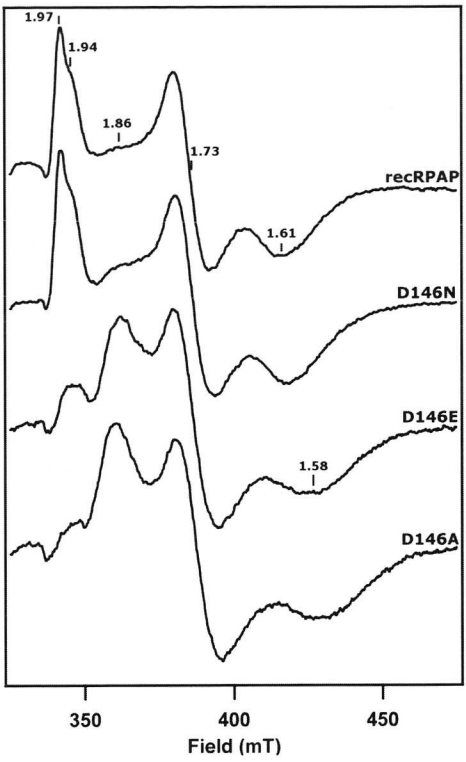

mixture of the intact and proteolytically cleaved wild-type enzyme, with a small g_z feature at 1.97-1.94 together with a major feature at g = 1.86. Except for the presence of a small g = 1.86 signal, the EPR spectrum of the D146N mutant was essentially identical to that of the wild-type enzyme. A weak copper signal around g = 2.05 was observed in all spectra. To investigate whether additional interactions are partially responsible for the low activity of the single polypeptide enzyme, cleavage of the mutant PAPs by proteases was performed. It has previously been demonstrated that the cysteine proteases papain and cathepsin B are more effective at activating RPAP than trypsin, and that cysteine proteases may be involved in proteolytic cleavage and activation of PAPs in vivo (9). Consequently, wild-type recRPAP and the D146N, D146E and D146A mutants were treated with cathepsin L, which results in even higher activation than cathepsin B (J. Ljusberg, G. Andersson, unpublished results); the results are presented in Table 3.1. After cathepsin L digestion, the k_{cat} of all PAP forms investigated was about the same magnitude (2000-2400 s^{-1}), which is approximately 8 fold higher than that of wild-type recRPAP. Since the activities reported in Table 3.1 were measured at higher temperature, and at a single, non-optimal pH, the values do not exactly parallel the k_{cat} values in Figure 3.3. The proteolytically cleaved recRPAPs were analyzed by Western blots in order to confirm the expected cleavage pattern and the absence of single polypeptide PAP. Cathepsin L treatment converted all of the 36 kDa PAP forms examined into forms with subunit masses of 20 kDa and 16 kDa, respectively (Figure 3.2).

Table 3.2: PAP activity[a] with OPN as substrate[b] at pH 5.8 and 37°C.

	Spec. Act. ($U\ mg^{-1}$)	k_{cat} (s^{-1})	Activation[c] (vs. wt recRPAP)	K_M (μM)	k_{cat}/Km ($*10^3\ M^{-1}*s^{-1}$)	Activation[d] (vs. wt recRPAP)
wt recRPAP	19.8	11.5	1	26.1	440.6	1
+ cat L	134.3	78.3	6.8	22.3	3511	8.0
D146A	37.8	22.0	1.9	9.4	2340	5.3
+ cat L	152.6	89.0	7.7	25.1	3546	8.0

[a] Activity measurements were performed as described in the experimental section under "kinetics measurements; osteopontin".
[b] Mean values from two experiments.
[c] Times activation of k_{cat}.
[d] Times activation of k_{cat}/K_M

Previous work showed that proteolytic cleavage of recRPAP with trypsin resulted in significantly less activation (*9*) than is observed for cleavage with cysteine proteases. Based on these results and MS experiments on recHPAP, we proposed that cleavage of a single peptide bond in the loop region results in a fragment that is held in place by noncovalent forces (*27*). To test this hypothesis, wild-type recRPAP and the D146A mutant were digested with trypsin. The activity of wild-type recRPAP increased 2.8 fold (268 versus 759 s^{-1}), while cleavage of the D146A mutant with trypsin gave no increase in activity (Table 3.2). Immunostained Western blots of the trypsin-digested preparations showed undetectable amounts of the single polypeptide forms (data not shown).

Based on the crystal structure of RPAP, it was proposed that the low enzymatic activity of the single polypeptide enzyme was due to steric interactions between the loop region and the substrate (*17*). The fact that the K_M value of a small (*p*-NPP) or a large (osteopontin, OPN) substrate molecule does not change significantly upon proteolysis of the enzyme indicates that steric effects are not responsible for the increase in activity observed upon proteolysis. To address this point directly, we examined the effect of proteolysis of wild-type recRPAP and the D146A mutant on their activity with a much bulkier substrate, the acidic phosphoprotein OPN, a putative *in vivo* substrate for PAP. The results (Table 3.2) show that cleavage by cathepsin increases the rate of hydrolysis of OPN 6.8-fold (11.5 versus 78.3 s^{-1}) for the wild-type protein and 4-fold (22.0 versus 89.0 s^{-1}) for the D146A mutant. Thus, comparable levels of activation are observed for both the wild-type enzyme and the D146A mutant with either *p*-NPP or OPN as substrate.

Based on the available crystal structures of mammalian PAPs, two specific interactions were suggested to be responsible for the differences between intact and proteolytically cleaved enzyme: that between Asp146 and His92, which primarily affects the water/hydroxide bound to Fe^{3+}; and that between Asp146 and Asn91, which decreases the Lewis acidity of the divalent metal ion, thereby decreasing the electrophilicity of a substrate bound to that (*27*). Because the EPR spectrum of the $Fe^{3+}Fe^{2+}$ form of recRPAP is due to an antiferromagnetically coupled system with an S = 1/2 ground state, it is difficult to correlate changes in the EPR spectrum with changes in the environment of the individual components of the binuclear center. Substitution of high-spin ferrous ion (S = 2) by a diamagnetic metal such as Zn^{2+} results in an EPR spectrum due to the magnetically isolated high-spin ferric ion (S = 5/2) (*37*). The FeZn form of recRPAP was therefore prepared, and the effect of proteolytic cleavage was examined.

Figure 3.5: EPR spectra of single polypeptide (A) and cathepsin L proteolytically cleaved (B) forms of FeZn-recRPAP. EPR conditions: microwave power 2 mW; microwave frequency, 9.42 GHz; Modulation, 12.7 G at 100 kHz; temperature, 4.6 K.

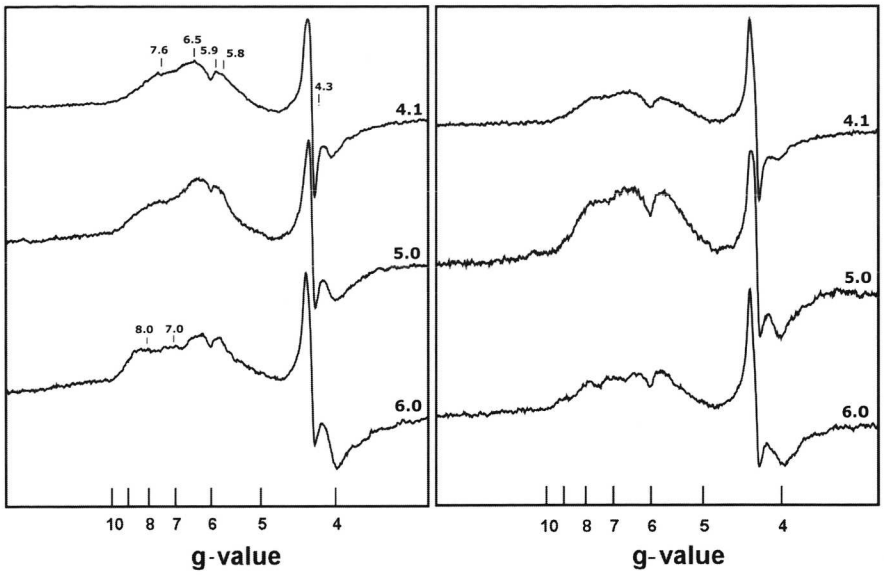

Intact FeZn-recRPAP had a λ_{max} of 525 nm, and its activity at pH 5.5 was considerably higher (800 s^{-1}) than that of the $Fe^{3+}Fe^{2+}$ protein (230 s^{-1}). The activity measured after incubation with H_2O_2 was the same as that measured in the presence of Fe^{2+}/ascorbate, indicating that significant amounts of the FeFe form were not present. Cleavage with cathepsin L produced fragments of m.w. 16 and 20 kDa, as shown by SDS-PAGE under reducing conditions. Kinetics measurements showed that proteolysis resulted in an increase in k_{cat} to 4200 s^{-1} at pH 6.2, with no change in K_M. As shown in Figure 3.5, the EPR spectra of intact and proteolytically cleaved FeZn-recRPAP are essentially identical over the range pH 4.1 to 6.0. At pH 4.1, the spectra of both show peaks due to a mixture of high-spin Fe^{3+} species with rhombicities of E/D = 0.02 (g = 6.5 and 5.9 for the ground and middle Kramer's doublets, respectively), E/D = 0.08 (g = 7.6 and 5.8 for the ground and middle Kramer's doublets, respectively), and E/D = 0.33 (g = 4.3). At pH 6.0, both intact and proteolytically cleaved recRPAP show additional features at g = 7.0 (E/D = 0.05) and g = 8.8 (E/D = 0.17). Thus, in contrast to $Fe^{3+}Fe^{2+}$-recRPAP, proteolysis of FeZn-recRPAP produces no changes in EPR spectra at pH 5.0.

Discussion

The mammalian purple acid phosphatases are single polypeptide or two-subunit enzymes with molecular masses of 36 kDa, and 20 and 16 kDa respectively. In addition, they differ in turnover number, pH optima, and EPR spectra at pH 5.0. The differences between these two species are due to proteolytic processing of an exposed loop near the active site (*9, 26, 27*), as can be seen by comparing the X-ray structures of rat bone PAP

at 2.2 Å (*17*) and 2.7 Å (*18*) resolution. In the latter structure, the loop region (residues 146 to 161 according to the human sequence (*38*)) is absent, while in the former structure it is present and well-resolved. Mass spectrometry of recombinant human PAP revealed that a portion of this loop is removed by trypsin digestion (*27*). Western blot analysis of recRPAP cleaved with various proteases showed different fragmentation patterns (*9*), suggesting a correlation between enzymatic activation and the extent of cleavage and/or the identity of the cleavage sites (vide infra).

Based on the recently published X-ray structures of Uf and recRPAP, an interaction between this loop and the active site was proposed to be responsible for the kinetics and spectroscopic differences observed for various mammalian PAPs (*27*). The carboxylate side chain of Asp146 is well positioned to hydrogen bond to the amido group of Asn91, a ligand to the ferrous ion. Although the orientation is less favorable, the Asp146 carboxylate can also interact with the imidazole group of His92, which is located near the ferric ion and has been proposed to be involved in substrate binding. Anologous residues have been shown to be important in the protein phosphatases, whose catalytic sites are very similar to those of the purple phosphatases. In the protein phosphatases, Asn91 is a ligand to one of the metal ions and it has been proposed to function in both catalysis and substrate coordination. Mutation of this residue to Asp, which is a better electron donor, results in a more acidic pH optimum and a decrease in activity. The Asn91Ala mutant shows a drastic decrease in catalytic activity, and the basic limb of the pH optimum was not observed in the pH versus activity plot (*39*). His92 of the protein phosphatases has been proposed to act as a general base catalyst that deprotonates an iron-coordinated solvent molecule (*25, 28*), but isotope effect studies have not yet confirmed this proposal (*40*).

In the present study, we prepared mutants of recRPAP in which the loop residue Asp146 was mutated to: Asn, whose neutral but polar side chain should interact more weakly with both Asn91 and His92; Glu, with a longer side chain that in principle could still interact with His92; and Ala, whose small nonpolar side chain should completely abolish this interaction. The properties of the Asp146Ala mutant convincingly show that the interaction of this residue of the loop region with the binuclear iron site is responsible for the lower catalytic activity and pH optimum and the more rhombic EPR spectrum of the single polypeptide wild-type enzyme. Moreover, these results show that activation does not depend upon the presence of the loop, which excludes relief of steric hindrance as an explanation for the activation phenomenon (*17*). Consistent with this observation is that the activation of both wild-type enzyme and Asp146Ala mutant upon proteolysis with cathepsin L does not depend on the size of the substrate. Although OPN is preferred to *p*-NPP as substrate, (as shown by the higher k_{cat}/K_M values), the catalytic activity increases by approximately 4-8 fold for both *p*-NPP and OPN upon proteolysis. K_M for OPN increases upon proteolysis, in contrast to the observed reduction in K_M for *p*-NPP, further supporting the conclusion that activation is an electrostatic rather than a steric effect.

The properties of the Asp146Asn mutant do indeed show that reducing the strength of the electrostatic interaction of this side chain with the active site increases the catalytic activity and makes the EPR spectrum more axial, as shown by the shoulder at g = 1.86. It cannot be completely excluded that part of the higher activity and the shoulder in the EPR spectrum of the Asp146Asn mutant are due to the presence of small quantities of proteolytically cleaved enzyme that were not detected with Coomassie staining. Based on

calculations using the specific activity of highly purified recRPAP (*9*), the proportion of proteolytically cleaved protein in the Asp146Asn should be approximately 15%, 8% for recRPAP, and 30-50% for the other mutants. Based on the SDS-PAGE results (Fig 3.1) this amount of proteolytically cleaved protein could very well be present in the wild-type protein, but not in the mutant proteins. In the Asp146Glu mutant, it is clear that both the enzymatic turnover number and the pH optimum are higher than in the wild-type enzyme, which correlates nicely with the shift in $pK_{es,1}$ to higher pH. On the other hand, the EPR spectrum of this mutant is more affected than would be expected based on the three-fold increase in activity. An explanation for this is provided by modeling of the three mutants in the Swiss-PdbViewer (http://www.expasy.ch/spdbv/mainpage.html by Glaxo Wellcome Experimental Research) and via Swiss-model (http://www.expasy.ch/swissmod/) (Figure 3.6). The modeled structure of the Asp146Glu mutant shows that the carboxylate side chain of the Glu points outward instead of inward toward the active site. Thus, the interaction with Asn91 is lost completely, but the distance between the carboxylate and His91 is unchanged (although the orientation for hydrogen bonding remains unfavorable). The structure of Uf (*16*) shows that water molecules are present in this region, which could form a hydrogen bonding network between the side chain and the iron site that affects the activity but not the Fe–Fe interaction, as shown by EPR spectra. Consequently, k_{cat} and the pH optimum might be expected to be affected less than the EPR spectrum, as is observed. These arguments imply that the interaction of Asp146 with Asn91 is more important than its interaction with His92, which is supported by the site-directed mutagenesis studies on PPs discussed above (*28, 39, 41, 42*).

To examine the nature of the Asp146-active site interactions in more detail, we prepared the FeZn form of recRPAP. The EPR spectrum of this species should be quite sensitive to changes at the Fe^{3+} site and relatively insensitive to changes at the Fe^{2+} site (*33*). Since it is known that proteolysis alters the EPR spectrum of FeFe-recHPAP at pH 5.0 (*27*) and FeFe-recRPAP (unpublished results, E.G. Funhoff, and B.A. Averill), the effect of proteolysis on the EPR spectrum of FeZn-recRPAP should allow us to distinguish between interactions with the trivalent and divalent metal sites. Proteolysis of FeZn-recRPAP with cathepsin L resulted in no significant changes in the EPR spectrum. This result strongly suggests that the interaction between the loop region and the active site primarily involves the Fe^{2+} site, presumably via hydrogen bonding between the Asp146 carboxylate group and the Asn91 amido group.

Since there is a relationship between the site of cleavage and the specific activity of proteolyzed PAPs (*9, 26, 27*), the effect of proteolysis of recRPAP mutants by trypsin and cathepsin L was examined. The sequence of recRPAP indicates the presence of only a single trypsin cleavage site (after Arg157), presumably resulting in a "tail" that is held in place by non-covalent forces. Cathepsin L, however, displays a broad hydrolytic activity, especially towards substrates with hydrophobic residues. Consequently, it is capable of cleaving the exposed loop region at several sites and possibly excising the entire loop, as supported by SDS-PAGE analysis (*9*). If the only relevant interactions are those between Asp146 and His92 or Asn91, trypsin or cathepsin L digestion should not affect the activity of the Asp146Ala mutant. As shown in Table 3.2, however, treatment of the Asp146Ala mutant with cathepsin L results in an almost two-fold increase in its enzymatic activity, while trypsin has no effect. Thus, interactions between other residues in the loop and the

Figure 3.6: Modeled 3-D orientation of residue Asp146 in wild-type and mutants Asp146Asn, Asp146Glu, and Asp146Ala using the program Swiss-PdbViewer by Glaxo Wellcome Experimental Research

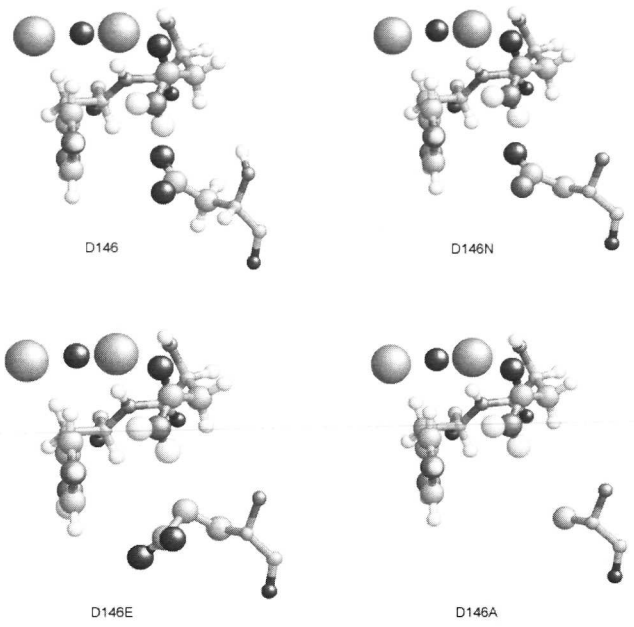

active site are also factors in the low catalytic activity observed for mammalian PAPs isolated as a single polypeptide.

Analysis of the interaction between the active site and the loop region of Uf and recRPAP with the program Chime (available at http://www.umass.edu/microbio/chime/find-ncb/index.html) showed that a hydrogen bonding network of water molecules is present in a cavity between the loop and the active site residues. This network results in additional interactions between the active site and the loop region, which could affect the enzymatic properties. In particular, hydrogen bonding of residues Gln151 and Gln152 via water can occur to either His195, postulated to be involved in binding the substrate, or to one of the oxygen atoms of a bridging phosphate. The distances between the side chains of these residues and the water molecules vary between 2.5 and 3.1 Å, within the range of hydrogen bonding. The presence of a hydrogen-bonding network of water molecules can also explain the difference between the effects of cleavage by cathepsin L and trypsin. Since cathepsin L appears to remove the entire loop region, the effects of hydrogen bonding with Gln151 and Gln152 are lost upon treatment with cathepsin L but not with trypsin. The side chain of Ser145 is also capable of interacting with Hiss221 and/or Asn91 (ligands to the Fe^{2+} ion, although less favorably). This residue is, however, present in the X-ray structure of proteolytically cleaved recRPAP at 2.7 Å resolution (*18*), indicating that it is not part of the portion that is removed upon proteolysis.

In conclusion, we have shown that the interaction between residue Asp146 of the loop region and (an) active site residue(s) is the major factor in the observed differences between single polypeptide and two-subunit forms of mammalian PAPs. Other

interactions, such as water-mediated hydrogen bonding between residues in the loop region and the active site, are also present but are less important. Interactions between the loop and the active site primarily affect the divalent metal ion, and loss of these interactions upon proteolysis results in altered kinetics and spectroscopic properties. These results are consistent with the proposal that the nucleophilic hydroxide bridges the two metal ions (*43-45*), as has also been proposed for binuclear Ni and Zn enzymes (*46-48*). Our results do not support a mechanism in which the nucleophilic hydroxide ion is terminally bound to the trivalent (ferric) site (*33, 49-53*), as has also been proposed for the PPs (*22, 23, 54*). Further studies on the identity of the nucleophile using different spectroscopic techniques are necessary to resolve this issue, and the differences between single polypeptide and proteolytically cleaved PAPs should be useful in this regard.

References

1. Klabunde, T., and Krebs, B. (1997) *Structure and Bonding 89*, 177-198.
2. Vogel, A., Spener, F., and Krebs, B. (2001) *Handbook of metalloproteins*, in press.
3. Schenk, G., Ge, Y. B., Carrington, L. E., Wynne, C. J., Searle, I. R., Carroll, B. J., Hamilton, S., and deJersey, J. (1999) *Arch. Biochem.Biophys. 370*, 183-189.
4. Schenk, G., Korsinczky, M. L. J., Hume, D. A., Hamilton, S., and DeJersey, J. (2000) *Gene 255*, 419-424.
5. Oddie, G. W., Schenk, G., Angel, N. Z., Walsh, N., Guddat, L. W., De Jersey, J., Cassady, A. I., Hamilton, S. E., and Hume, D. A. (2000) *Bone 27*, 575-584.
6. Vallet, J. L., Christenson, R. K., and Mcguire, W. J. (1996) *Biol Reprod 55*, 1172-1178.
7. Buhi, W. C., Ducsay, C. A., Bazer, F. W., and Roberts, R. M. (1982) *J. Biol. Chem. 257*, 1712-1723.
8. Hayman, A. R., Warburton, M. J., Pringle, J. A. S., Coles, B., and Chambers, T. J. (1989) *Biochem. J. 261*, 601-609.
9. Ljusberg, J., EkRylander, B., and Andersson, G. (1999) *Biochem. J. 343*, 63-69.
10. Hayman, A. R., Jones, S. J., Boyde, A., Foster, D., Colledge, W. H., Carlton, M. B., Evans, M. J., and Cox, T. M. (1996) *Development 122*, 3151-3162.
11. Angel, N. Z., Walsh, N., Forwood, M. R., Ostrowski, M. C., Cassady, A. I., and Hume, D. A. (2000) *J. Bone Miner. Res. 15*, 103-110.
12. Hayman, A. R., Bune, A. J., Bradley, J. R., Rashbass, J., and Cox, T. M. (2000) *J. Histochem. Cytochem. 48*, 219-227.
13. Andersson, G., and EkRylander, B. (1995) *Acta Orthopaedica Scandinavica 66*, 189-194.
14. Ashkar, S., Weber, G. F., Panoutsakopoulou, V., Sanchirico, M. E., Jansson, M., Zawaideh, S., Rittling, S. R., Denhardt, D. T., Glimcher, M. J., and Cantor, H. (2000) *Science 287*, 860-864.
15. Sträter, N., Klabunde, T., Tucker, P., Witzel, H., and Krebs, B. (1995) *Science 268*, 1489-1492.
16. Guddat, L. W., McAlpine, A. S., Hume, D., Hamilton, S., de Jersey, J., and Martin, J. L. (1999) *Structure with Folding & Design 7*, 757-767.
17. Lindqvist, Y., Johansson, E., Kaija, H., Vihko, P., and Schneider, G. (1999) *J. Mol. Biol. 291*, 135-147.
18. Uppenberg, J., Lindqvist, F., Svensson, C., EkRylander, B., and Andersson, G. (1999) *J. Mol. Biol. 290*, 201-211.
19. Durmus, A., Eicken, C., Spener, F., and Krebs, B. (1999) *Biochim. Biophys.Acta-Protein Structure and Molecular Enzymology 1434*, 202-209.
20. Kissinger, C. R., Parge, H. E., Knighton, D. R., Lewis, C. T., Pelletier, L. A., Tempczyk, A., Kalish, V. J., Tucker, K. D., Showalter, R. E., Moomaw, E. W., Gastinel, L. N., Habuka, N., Chen, X., Maldonado, F., Barker, J. E., Bacquet, R., and Villafranca, J. E. (1995) *Nature 378*, 641-644.
21. Goldberg, J., Huang, H.-B., Kwon, Y.-G., Greengard, P., Nairn, A. C., and Kuriyan, J. (1995) *Nature 376*, 745-753.
22. Egloff, M. P., Cohen, P. T. W., Reinemer, P., and Barford, D. (1995) *J. Mol. Biol. 254*, 942-959.
23. Griffith, J. P., Kim, J. L., Kim, E. E., Sintchak, M. D., Thomson, J. A., Fitzgibbon, M. J., Fleming, M. A., Caron, P. R., Hsiao, K., and Navia, M. A. (1995) *Cell 82*, 507-522.
24. Vincent, J. B., Averill, B. A. (1990) *FEBS 263*, 265-268.
25. Rusnak, F., and Mertz, P. (2000) *Physiol. Rev. 80*, 1483-1521.
26. Orlando, J. L., Zirino, T., Quirk, B. J., and Averill, B. A. (1993) *Biochemistry 32*, 8120-8129.
27. Funhoff, E. G., Klaassen, C. H. W., Samyn, B., Van Beeumen, J., and Averill, B. A. (2001) *ChemBioChem 2*, 355-363.
28. Mertz, P., Yu, L., Sikkink, R., and Rusnak, F. (1997) *J. Biol. Chem. 272*, 21296-21302.
29. Ek-Rylander, B., Barkhem, T., Ljusberg, J., Ohman, L., Andersson, K. K., and Andersson, G. (1997) *Biochem J 321*, 305-311.
30. Laemmli, U. K. (1970) *Nature 227*, 680-685.
31. Baykov, A. A., Evtushenko, O. A., and Avaeva, S. M. (1988) *Anal. Biochem. 171*, 266-270.
32. Merkx, M., and Averill, B. A. (1998) *Biochemistry 37*, 11223-11231.
33. Merkx, M., Pinkse, M. W. H., and Averill, B. A. (1999) *Biochemistry 38*, 9914-9925.

34. Segel, I. H. (1993) *Enzyme Kinetics: Behaviour and analysis of rapid equilibrium and steady-state enzyme systems*, John Wiley & Sons, New York.
35. Sinn, E., O'Connor, C. J., de Jersey, J., and Zerner, B. (1983) *Inorg. Chim. Acta 78*, L13-L15.
36. Debrunner, P. G., Hendrich, M. P., de Jersey, J., Keough, D. T., Sage, J. T., and Zerner, B. (1983) *Biochim. Biophys. Acta 745*, 103-106.
37. Davis, J. C., and Averill, B. A. (1982) *Proc. Natl. Acad. Sci. USA 79*, 4623-4627.
38. Lord, D. K., Cross, N. C. P., Bevilacqua, M. A., Rider, S. H., Gorman, P. A., Groves, A. V., Moss, D. W., Sheer, D., and Cox, T. M. (1990) *Eur. J. Biochem. 189*, 287-293.
39. Zhang, J., Zhang, Z. J., Brew, K., and Lee, E. Y. C. (1996) *Biochemistry 35*, 6276-6282.
40. Hoff, R. H., Mertz, P., Rusnak, F., and Hengge, A. C. (1999) *J. Am. Chem. Soc. 121*, 6382-6390.
41. Zhuo, S., Clemens, J. C., Stones, R. L., and Dixon, J. E. (1994) *J. Biol. Chem. 269*, 26234-26238.
42. Huang, H. B., Horiuchi, A., Goldberg, J., Greengard, P., and Nairn, A. C. (1997) *Proc.Natl. Acad. Sci.USA 94*, 3530-3535.
43. Wang, X. D., Ho, R. Y. N., Whiting, A. K., and Que, L. (1999) *J. Am. Chem.Soc. 121*, 9235-9236.
44. Yang, Y. S., McCormick, J. M., and Solomon, E. I. (1997) *J. Am. Chem. Soc. 119*, 11832-11842.
45. Wang, X., Randall, C. R., True, A. E., and Que, L., Jr. (1996) *Biochemistry 35*, 13946-13954.
46. Yamaguchi, K., Cosper, N. J., Stalhandske, C., Scott, R. A., Pearson, M. A., Karplus, P. A., and Hausinger, R. P. (1999) *J. Biol. Inorg. Chem. 4*, 468-477.
47. Benini, S., Rypniewski, W. R., Wilson, K. S., Miletti, S., Ciurli, S., and Mangani, S. (2000) *J. Biol. Inorg. Chem. 5*, 110-118.
48. Carfi, A., Duee, E., PaulSoto, R., Galleni, M., Frere, J. M., and Dideberg, O. (1998) *Acta Crystallographica Section D: Biological Crystallography 54*, 47-57.
49. Dietrich, M., Münstermann, D., Suerbaum, H., and Witzel, H. (1991) *Eur. J. Biochem. 199*, 105-113.
50. Aquino, M. A. S., Lim, J.-S., and Sykes, A. G. (1994) *J. Chem. Soc. Dalton Trans.*, 429-436.
51. Pinkse, M. W. H., Merkx, M., and Averill, B. A. (1999) *Biochemistry 38*, 9926-9936.
52. Merkx, M., and Averill, B. A. (1999) *J. Am. Chem. Soc. 121*, 6683-6689.
53. Klabunde, T., Sträter, N., Fröhlich, R., Witzel, H., and Krebs, B. (1996) *J. Mol. Biol. 259*, 737-748.
54. Voegtli, W. C., White, D. J., Reiter, N. J., Rusnak, F., and Rosenzweig, A. C. (2000) *Biochemistry 39*, 15365-15374.